Learning-based sound-speed correction for dual-modal photoacoustic/ultrasound imaging

Mengjie Shi*, Tom Vercauteren, and Wenfeng Xia
School of Biomedical Engineering and Imaging Sciences, King's College London, London, UK
*Email: mengjie.shi@kcl.ac.uk

***Abstract*— Accurate determination of the speed-of-sound (SoS) within the propagation medium is of significant importance in photoacoustic (PA) image reconstruction. A common practice in PA imaging assumes a homogeneous SoS distribution, e.g., 1540 m/s for soft tissue similar to that implemented in conventional ultrasound (US) beamforming. This assumption can lead to US aberration artefacts that degrade the image quality due to tissue heterogeneity. In this work, we introduce a learning-based method focusing on compensating SoS variations for PA image reconstruction in a dual-modal PA/US imaging system. Deep neural networks were trained for SoS retrieval using US channel data and subsequently informed the corresponding PA image reconstruction. The proposed framework demonstrated effective mitigation of US aberration artefacts with a numerical phantom, achieving a structural similarity index measure of 0.8267 compared to 0.5042 with the conventional SoS assumption of 1540 m/s. Likewise, the enhancements were also evident when testing the framework with ex vivo US/PA data, implying its great potentials in improving PA image quality for in vivo applications.**

Keywords*— *Photoacoustic imaging, Ultrasound imaging, Ultrasound aberration, speed-of-sound, deep learning

I. Introduction

PA imaging is a hybrid imaging modality based on optical absorption and US detection. Capitalising on rich optical spectroscopic contrast and deep US imaging depth at ultrasonic resolution, PA imaging has been widely investigated for various pre-clinical and clinical applications [1]–[3]. In PA tomography, PA images are reconstructed via an acoustic inversion algorithm, i.e., acoustic waves detected by US transducers can be backpropagated to reconstruct initial pressure distributions. Similar to US beamforming, SoS in the propagation medium needs to be specified and a constant SoS value of 1540 m/s is commonly assumed. However, this assumption is readily disrupted in practice, as tissues exhibit heterogeneity. Failure to compensate SoS variations can lead to serve aberration artefacts that deteriorate the image quality.

Researchers have explored different ways to mitigate sound speed aberrations in PA image reconstruction. SoS can be globally optimised regarding image fidelity metrics like image sharpness [4] and coherent factor [5]. But these methods fall short of accounting for local SoS variations. In contrast, a joint reconstruction (JR) problem was established seeking for concurrently retrieving SoS distributions and initial pressure distributions (or optical absorption maps) from PA measurements [6]–[9]. On the other hand, SoS maps can be rigorously measured with dual-modal PA/US imaging systems combing US transmission tomography and PA tomography [10]–[12]. However, such imaging systems are generally associated with hardware sophistication and substantial computation requirements. Deep learning (DL) has made noticeable advancements in signal and image processing in the field of US and PA imaging. For instance, Jeon et al. introduced a DL based method using simulated PA data for SoS aberration mitigation and artefact removal [13]. It was noted that the training dataset was simulated based on the assumption that SoS was largely homogeneous, which may be deficient for highly heterogeneous tissues.

In this work, we propose a learning-based method for SoS compensation based on a dual-modal linear array-based US/PA imaging system.

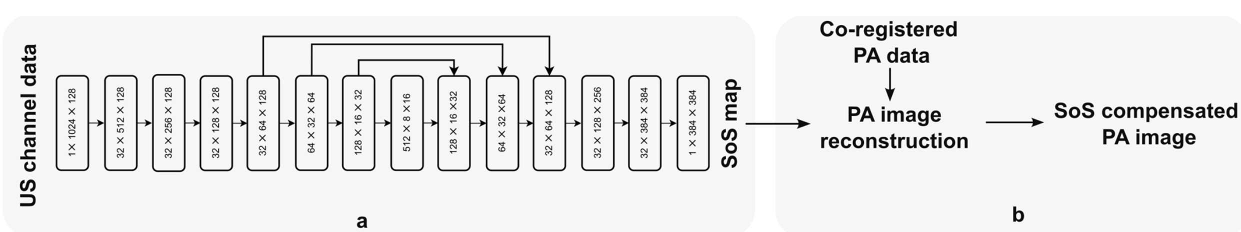

Fig. 1 Schematic diagram of a learning-based framework for speed-of-sound (SoS) reconstruction (a) and compensation (b) in dual-modal photoacoustic (PA) /ultrasound (US) imaging.

II. Materials and Methods

The proposed framework was schematically shown in Fig. 1, deep neural networks were trained to reconstruct SoS distributions from US channel data, which were utilised for PA reconstruction via a time-reversal algorithm [14]. The initial evaluation of the proposed method was performed with numerical phantoms containing unseen layered structures, and ex vivo tissues in comparison with the conventional approach where a homogeneous SoS of 1540 m/s for soft tissue was assumed.

A. *Dataset preparation*

The training dataset was generated from US simulations in k-Wave where the acquisition parameters were modelled based on a clinical US probe used in a dual-modal linear array-based PA/US imaging system (AcousticX, Cyberdyne INC.) [15]–[18]. The probe had a total number of 128 elements spanning a length of 38.4 mm with a central frequency of 7 MHz and a pitch size of 0.3 mm. Structures in US images were simulated as homogenous backgrounds with the elliptical inclusions mimicking organs and lesions. SoS values for the background and inclusions were randomly chosen from a uniform distribution ranging from 1400 m/s to 1600 m/s. Acoustic attenuation and mass intensity was fixed to 0.5 dB/MHz/cm and 1020 kg/m3. The speckle density had a mean distribution of 3 speckles per λ square and the intensity deviation was uniformly sampled from -0.03 to 0.03. Thermal noise and electrical noise were also considered.

B. *Network Implementation*

As shown in Fig. 1a, the deep learning model was based on a fully convolutional neural network that maps an US raw data with dimensions of 1024×128 to the corresponding SoS distribution with a size of 384×384 (in number of pixels). The model was implemented using Keras 2.12.0 with Python 3.10.11. Training was performed on 2000 samples for 100 epochs with a batch size of 10 that minimised Mean Square Error (MSE) Loss using stochastic gradient descent (SGD) optimizer. The experiments were conducted on NVIDIA DGX cluster equipped with 8 A100 GPUs.

III. Results

A. *Numerical phantom*

The trained model was tested on in silico PA/US data obtained from a numerical phantom as shown in Fig. 3. The phantom consisted of two layers with a homogenous SoS of 1406 m/s and 1553 m/s for each layer, respectively. Fig. 3c shows the SoS map predicted by the DL method with an average SoS of 1411 m/s for the first layer and 1533 m/s for the second layer. The predicted SoS map was incorporated in PA image reconstruction in comparison with a conventional SoS assumption of 1540 m/s and ground truth SoS, as shown in Fig. 3e-g. US aberration artefacts manifesting as arc-shaped signals (shown in the insets) were observed in the conventional reconstruction at all depths. In contrast, the DL-based method effectively suppressed the aberration artefacts (structural similarity index measure: 0.8267 vs 0.5042 with the conventional reconstruction). The enhancement was consistent at depths of up to around 3 cm.

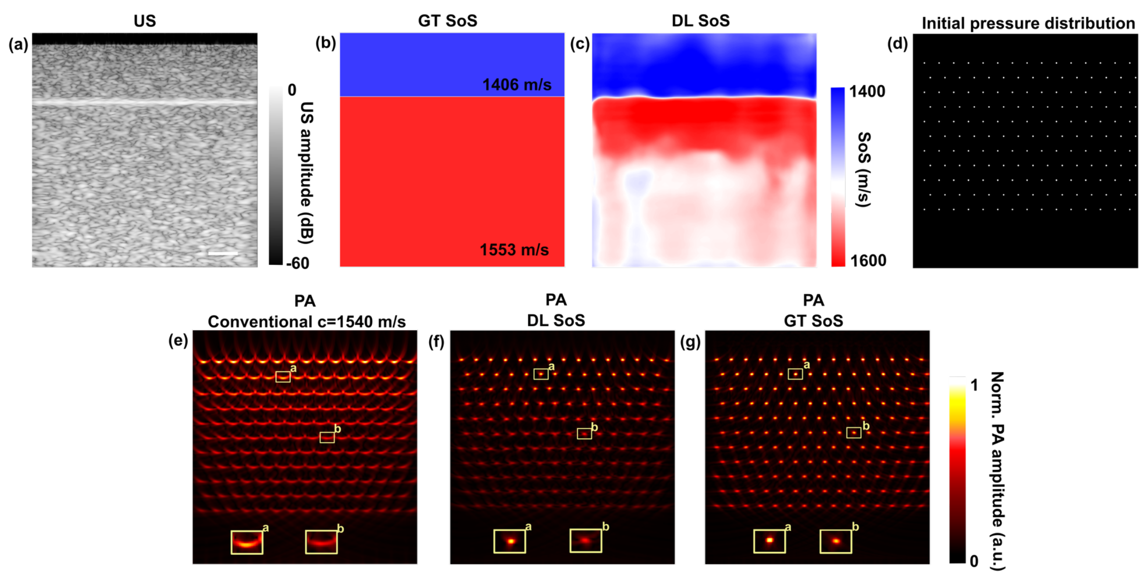

Fig. 3 Evaluation of deep learning (DL) -based speed-of-sound (SoS) compensation method using in silico photoacoustic (PA)/ ultrasound (US) data. GT: ground truth. Scale bar: 5.00 mm. PA images were normalised regarding the individual maximum amplitude.

B. *Chicken breast tissue ex vivo*

To further test the generalisation ability of the DL model, ex vivo PA/US data were prepared from an ex vivo tissue phantom made of fresh chicken breast tissues and two pencil leads with the same diameter of 0.5 mm. As shown in Fig. 3b, the SoS difference between the coupling medium (water) and the tissues was successfully detected by the model. The averaged SoS estimation errors for the water and tissue regions (at depths of no more than 25 mm) were 11 m/s, 15 m/s, respectively (SoS of water was 1480 m/s at room temperature and soft tissue was 1540 m/s [19]). The corresponding SoS-compensated PA images were remarkably enhanced, as evidenced by the decrease in lateral resolution shown in Fig. 3f.

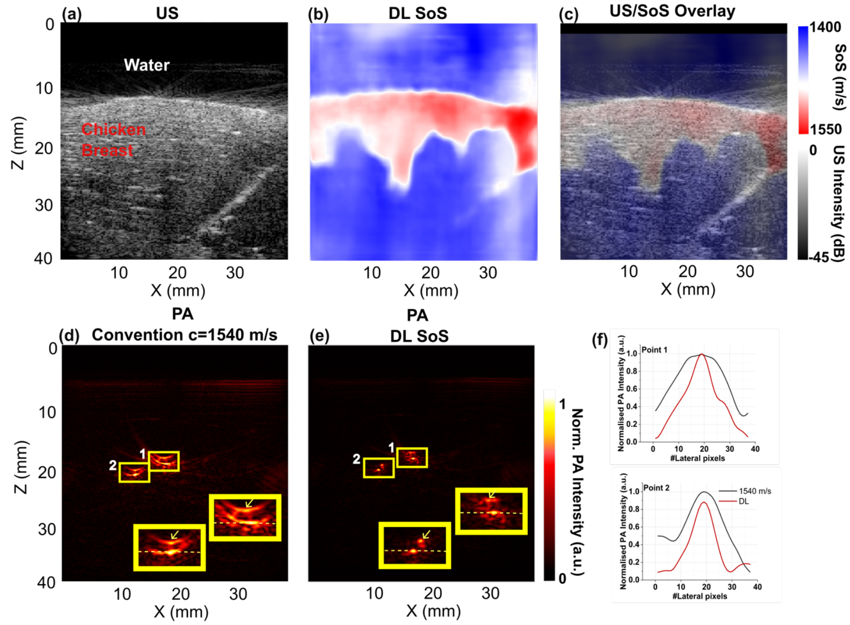

Fig. 3 Evaluation of deep learning (DL)-based speed-of-sound (SoS) compensation method using ex vivo photoacoustic (PA)/ ultrasound (US) data. Profiles in (f) were drawn along the yellow dashed lines. Reflection artefacts were denoted by the yellow arrows. A 2 mm offset was introduced on the DL SoS before shown in the overlay. PA images were normalised regarding the individual maximum amplitude.

IV. DISCUSSION & CONCLUSIONS

In this work, we explored the usage of DL for SoS compensation in PA image reconstruction using co-registered US channel data in a dual-modal PA/US imaging system. This was inspired by recent studies investigating the feasibility of reconstructing SoS distributions directly from US channel data using DL models [20]–[22]. The proposed framework was tested using unseen in silico data and ex vivo data. The DL model was able to detect the SoS heterogeneity of the numerical phantom and ex vivo tissues using US channel data. The incorporation of SoS distribution effectively reduced the aberration artefacts in PA images. For the numerical phantom, the similarity index measure was improved by around 66% in contrast to the homogeneous SoS of 1540 m/s adopted in the conventional beamforming. Hence, the proposed SoS compensation method can be potentially helpful in enhancing PA image quality for diverse in vivo applications.

ACKNOWLEDGMENT

This research was funded in whole, or in part, by Wellcome Trust [203148/Z/16/Z], EPSRC [NS/A000049/1] and King's – China Scholarship Council PhD Scholarship program (K-CSC) [202008060071].

REFERENCES

[1] P. Beard, "Biomedical photoacoustic imaging," *Interface Focus*, vol. 1, no. 4, pp. 602–631, Aug. 2011, doi: 10.1098/rsfs.2011.0028.

[2] T. Zhao, A. E. Desjardins, S. Ourselin, T. Vercauteren, and W. Xia, "Minimally invasive photoacoustic imaging: Current status and future perspectives," *Photoacoustics*, vol. 16, p. 100146, Dec. 2019, doi: 10.1016/j.pacs.2019.100146.

[3] L. V. Wang and J. Yao, "A practical guide to photoacoustic tomography in the life sciences," *Nat Methods*, vol. 13, no. 8, pp. 627–638, Aug. 2016, doi: 10.1038/nmeth.3925.

[4] B. E. Treeby, T. K. Varslot, E. Z. Zhang, J. G. Laufer, and P. C. Beard, "Automatic sound speed selection in photoacoustic image reconstruction using an autofocus approach," *JBO*, vol. 16, no. 9, p. 090501, Sep. 2011, doi: 10.1117/1.3619139.

[5] C. Yoon, J. Kang, S. Han, Y. Yoo, T.-K. Song, and J. H. Chang, "Enhancement of photoacoustic image quality by sound speed correction: ex vivo evaluation," *Opt. Express*, vol. 20, no. 3, p. 3082, Jan. 2012, doi: 10.1364/OE.20.003082.

[6] H. Jiang, Z. Yuan, and X. Gu, "Spatially varying optical and acoustic property reconstruction using finite-element-based photoacoustic tomography," *J. Opt. Soc. Am. A*, vol. 23, no. 4, p. 878, Apr. 2006, doi: 10.1364/JOSAA.23.000878.

[7] J. Zhang and M. A. Anastasio, "Reconstruction of speed-of-sound and electromagnetic absorption distributions in photoacoustic tomography," in *Photons Plus Ultrasound: Imaging and Sensing 2006: The Seventh Conference on Biomedical Thermoacoustics, Optoacoustics, and Acousto-optics*, SPIE, Mar. 2006, pp. 339–345. doi: 10.1117/12.647665.

[8] C. Huang, K. Wang, R. W. Schoonover, L. V. Wang, and M. A. Anastasio, "Joint Reconstruction of Absorbed Optical Energy Density and Sound Speed Distributions in Photoacoustic Computed Tomography: A Numerical Investigation," *IEEE Trans Comput Imaging*, vol. 2, no. 2, pp. 136–149, Jun. 2016, doi: 10.1109/TCI.2016.2523427.

[9] T. P. Matthews, J. Poudel, L. Li, L. V. Wang, and M. A. Anastasio, "Parameterized joint reconstruction of the initial pressure and sound speed distributions for photoacoustic computed tomography," *SIAM J Imaging Sci*, vol. 11, no. 2, pp. 1560–1588, 2018, doi: 10.1137/17M1153649.

[10] S. Manohar, R. G. H. Willemink, F. van der Heijden, C. H. Slump, and T. G. van Leeuwen, "Concomitant speed-of-sound tomography in photoacoustic imaging," *Applied Physics Letters*, vol. 91, no. 13, p. 131911, Sep. 2007, doi: 10.1063/1.2789689.

[11] J. Jose *et al.*, “Passive element enriched photoacoustic computed tomography (PER PACT) for simultaneous imaging of acoustic propagation properties and light absorption,” *Opt. Express, OE*, vol. 19, no. 3, pp. 2093–2104, Jan. 2011, doi: 10.1364/OE.19.002093.

[12] E. Merčep, J. L. Herraiz, X. L. Deán-Ben, and D. Razansky, “Transmission–reflection optoacoustic ultrasound (TROPUS) computed tomography of small animals,” *Light Sci Appl*, vol. 8, no. 1, Art. no. 1, Jan. 2019, doi: 10.1038/s41377-019-0130-5.

[13] S. Jeon, W. Choi, B. Park, and C. Kim, “A Deep Learning-Based Model That Reduces Speed of Sound Aberrations for Improved In Vivo Photoacoustic Imaging,” *IEEE Transactions on Image Processing*, vol. 30, pp. 8773–8784, 2021, doi: 10.1109/TIP.2021.3120053.

[14] B. E. Treeby, E. Z. Zhang, and B. T. Cox, “Photoacoustic tomography in absorbing acoustic media using time reversal,” *Inverse Problems*, vol. 26, no. 11, p. 115003, Nov. 2010, doi: 10.1088/0266-5611/26/11/115003.

[15] W. Xia *et al.*, “Handheld Real-Time LED-Based Photoacoustic and Ultrasound Imaging System for Accurate Visualization of Clinical Metal Needles and Superficial Vasculature to Guide Minimally Invasive Procedures,” *Sensors*, vol. 18, no. 5, Art. no. 5, May 2018, doi: 10.3390/s18051394.

[16] M. Shi *et al.*, “Enhanced Photoacoustic Visualisation of Clinical Needles by Combining Interstitial and Extracorporeal Illumination of Elastomeric Nanocomposite Coatings,” *Sensors*, vol. 22, no. 17, Art. no. 17, Jan. 2022, doi: 10.3390/s22176417.

[17] M. Shi, T. Vercauteren, and W. Xia, “Spatiotemporal singular value decomposition for denoising in photoacoustic imaging with a low-energy excitation light source,” *Biomed. Opt. Express, BOE*, vol. 13, no. 12, pp. 6416–6430, Dec. 2022, doi: 10.1364/BOE.471198.

[18] M. Shi, T. Zhao, S. J. West, A. E. Desjardins, T. Vercauteren, and W. Xia, “Improving needle visibility in LED-based photoacoustic imaging using deep learning with semi-synthetic datasets,” *Photoacoustics*, vol. 26, p. 100351, Jun. 2022, doi: 10.1016/j.pacs.2022.100351.

[19] J. Mamou and M. L. Oelze, Eds., *Quantitative Ultrasound in Soft Tissues*. Dordrecht: Springer Netherlands, 2013. doi: 10.1007/978-94-007-6952-6.

[20] M. Feigin, D. Freedman, and B. W. Anthony, “A Deep Learning Framework for Single-Sided Sound Speed Inversion in Medical Ultrasound,” *IEEE Transactions on Biomedical Engineering*, vol. 67, no. 4, pp. 1142–1151, Apr. 2020, doi: 10.1109/TBME.2019.2931195.

[21] F. K. Jush, M. Biele, P. M. Dueppenbecker, O. Schmidt, and A. Maier, “DNN-based Speed-of-Sound Reconstruction for Automated Breast Ultrasound,” in *2020 IEEE International Ultrasonics Symposium (IUS)*, Sep. 2020, pp. 1–7. doi: 10.1109/IUS46767.2020.9251579.

[22] F. Khun Jush, P. M. Dueppenbecker, and A. Maier, “Data-Driven Speed-of-Sound Reconstruction for Medical Ultrasound: Impacts of Training Data Format and Imperfections on Convergence,” in *Medical Image Understanding and Analysis*, B. W. Papież, M. Yaqub, J. Jiao, A. I. L. Namburete, and J. A. Noble, Eds., in Lecture Notes in Computer Science. Cham: Springer International Publishing, 2021, pp. 140–150. doi: 10.1007/978-3-030-80432-9_11.